Article

Cell Reports

Hand2 Is an Essential Regulator for Two Notch-Dependent Functions within the Embryonic Endocardium

Graphical Abstract

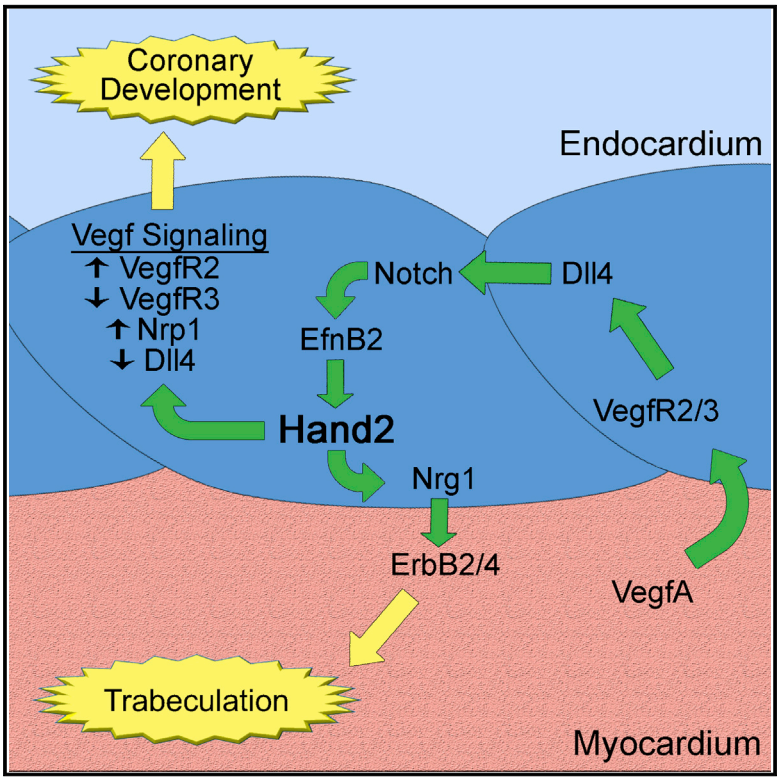

Authors

Nathan J. VanDusen, Jose Casanovas, ..., Weinian Shou, Anthony B. Firulli

Correspondence

tfirulli@iu.edu

In Brief

VanDusen et al. demonstrate that the bHLH transcription factor Hand2 is a critical mediator of Notch signaling within the embryonic endocardium regulating trabeculation, septation, and coronary formation. Endocardial loss of Hand2 causes tricuspid atresia, multiple ventricular septa, and hypervascularized myocardium, establishing Hand2-dependent endocardial-myocardial signaling as essential for cardiac morphogenesis.

Highlights

- *Hand2* endocardial ablation results in tricuspid atresia
- Hand2 mediates Notch and Ephrin signaling in the heart
- Hand2 modulates coronary development via regulation of Vegf signaling

VanDusen et al., 2014, Cell Reports *9*, 1–13
December 24, 2014 ©2014 The Authors
http://dx.doi.org/10.1016/j.celrep.2014.11.021

CellPress

Please cite this article in press as: VanDusen et al., Hand2 Is an Essential Regulator for Two Notch-Dependent Functions within the Embryonic Endocardium, Cell Reports (2014), http://dx.doi.org/10.1016/j.celrep.2014.11.021

Cell Reports
Article

Hand2 Is an Essential Regulator for Two Notch-Dependent Functions within the Embryonic Endocardium

Nathan J. VanDusen,[1] Jose Casanovas,[1] Joshua W. Vincentz,[1] Beth A. Firulli,[1] Marco Osterwalder,[2] Javier Lopez-Rios,[2] Rolf Zeller,[2] Bin Zhou,[3] Joaquim Grego-Bessa,[4] José Luis De La Pompa,[5] Weinian Shou,[1] and Anthony B. Firulli[1,*]
[1]Riley Heart Research Center, Wells Center for Pediatric Research, Departments of Pediatrics and Medical and Molecular Genetics, Indiana University, Indianapolis, IN 46202, USA
[2]Developmental Genetics, Department of Biomedicine, University of Basel, 4058 Basel, Switzerland
[3]Department of Genetics, Albert Einstein College of Medicine, New York, NY 10461, USA
[4]Department of Developmental Biology, Memorial Sloan Kettering Cancer Center, New York, NY 10021, USA
[5]Cardiovascular Developmental Biology Program, Cardiovascular Development and Repair Department, Centro Nacional de Investigaciones Cardiovasculares (CNIC), Madrid 28029, Spain
*Correspondence: tfirulli@iu.edu
http://dx.doi.org/10.1016/j.celrep.2014.11.021

SUMMARY

The basic-helix-loop-helix (bHLH) transcription factor Hand2 plays critical roles during cardiac morphogenesis via expression and function within myocardial, neural crest, and epicardial cell populations. Here, we show that Hand2 plays two essential Notch-dependent roles within the endocardium. Endocardial ablation of *Hand2* results in failure to develop a patent tricuspid valve, intraventricular septum defects, and hypotrabeculated ventricles, which collectively resemble the human congenital defect tricuspid atresia. We show endocardial Hand2 to be an integral downstream component of a Notch endocardium-to-myocardium signaling pathway and a direct transcriptional regulator of *Neuregulin1*. Additionally, Hand2 participates in endocardium-to-endocardium-based cell signaling, with *Hand2* mutant hearts displaying an increased density of coronary lumens. Molecular analyses further reveal dysregulation of several crucial components of Vegf signaling, including *VegfA*, *VegfR2*, *Nrp1*, and *VegfR3*. Thus, Hand2 functions as a crucial downstream transcriptional effector of endocardial Notch signaling during both cardiogenesis and coronary vasculogenesis.

INTRODUCTION

In the primitive heart, communication between the endocardium, which is the endothelium-like tissue that lines the heart, and the myocardium, which is the muscular heart tissue, is essential for processes central to normal cardiac morphogenesis, including trabeculation, chamber septation, and coronary vasculogenesis (Bruneau, 2003; Brutsaert, 2003). The transmembrane receptor Notch1 is integral to this communication, as endocardial Notch activates endocardial EphrinB2, which through unknown mechanisms activates expression of the secreted factor Neurgulin1 (*Nrg1*). Nrg1 initiates the trabeculation process, and Notch signaling subsequently activates expression of Bmp10 (Chen et al., 2004) through a separate pathway (Grego-Bessa et al., 2007). Bmp10 expression stimulates proper proliferation of trabecular, and possibly septal, myocardium. Disruption of Notch-mediated endocardial-myocardial communication results in congenital heart defects (CHDs), which are the most frequent human developmental anomalies (Hoffman, 1995).

Tricuspid atresia (TA) is a CHD characterized by the lack of a direct connection between the right atria (RA) and the right ventricle (RV), requiring both ventricular (VSD) and atrial (ASD) septal defects for embryonic survival (Anderson et al., 1979). Conditional ablation of the basic-helix-loop-helix (bHLH) factor *Hand2* within the second heart field (SHF) via *Mef2c-Cre* results in TA (Tsuchihashi et al., 2011). *Mef2c-Cre* marks a pool of SHF progenitor cells that contribute to both the myocardium and endocardium (Tsuchihashi et al., 2011; Verzi et al., 2005), and SHF ablation of Hand2 causes TA via unknown mechanisms. As cardiomyocyte-specific ablation of *Hand2* does not result in TA (Tsuchihashi et al., 2011), we hypothesized that loss of Hand2 function within the endocardium is causative of TA. Indeed, our data reveal that either endothelial or endocardial-specific deletion of *Hand2* (*H2CKO*) using either *Tie2-Cre* or *Nfatc1*^{Cre}, respectively, results in TA. These data show that Hand2 functions downstream of endocardial Notch to mediate endocardium-to-myocardium signaling via direct transcriptional regulation of the growth factor *Neuregulin1* (*Nrg1*).

As cardiogenesis proceeds, development of the coronary vasculature allows for oxygenation of the thickening ventricular compact zone. Cardiac endothelial cells form the primitive coronary network by angiogenesis (Red-Horse et al., 2010; Wu et al., 2012), a process that extracardiac models demonstrate to be Notch dependent. Early embryonic lethality in Notch pathway mutants has precluded robust analysis of Notch signaling in

coronary development. Significantly, *H2CKO* mice survive long enough to assess the initiation of coronary vascularization, and our findings indicate that Hand2 modulates coronary development through regulation of multiple Vegf signaling components within the developing heart. Collectively, these data support a model whereby Notch signaling, via endocardial Hand2 function, regulates trabeculation, interventricular septum (IVS) formation, and coronary development.

RESULTS

Endothelial/Endocardial Loss of Hand2 Causes Trabeculation and Septation Defects that Resemble Tricuspid Atresia

To test the hypothesis that loss of endocardial *Hand2* results in TA, we intercrossed the endothelial cell-specific *Tie2-Cre* allele (Kisanuki et al., 2001) with mice carrying the *Hand2* conditional allele (*Hand2^{fx}*). *Tie2-Cre* is expressed in all endothelial cells, including cells of the ventricular endocardium, coronary endothelium, and atrioventricular cushions (Kisanuki et al., 2001). *Tie2-Cre* expression initiates at embryonic day 8.5 (E8.5) (Kisanuki et al., 2001), which is concurrent with the onset of endocardial *Hand2* expression (Barnes et al., 2011). *Hand2$^{fx/fx}$;R26R^{lacZ}* females were mated with *Tie2-Cre(+);Hand2$^{+/-}$* males, and neonates were genotyped. No *H2CKO* mice were observed (n = 58; Table S1). We next set up timed matings and observed that *Tie2-Cre(+);Hand2$^{fx/-}$* embryos die by E14.5 (Table S1). *Hand2* deletion within the endocardium is evident by in situ hybridization (ISH) at E10.5 (Figures 1A and 1B, arrows). Examination of *Tie2-Cre H2CKOs* in whole mount (Figures 1D and 1E) and in section histology (Figures 1G and 1H) reveals hypotrabeculation (arrow in Figure 1E) and a highly penetrant TA phenotype (Figure 1H; Table S2) comparable to that reported in the SHF *Mef2c-Cre H2CKOs*. At E12.5, we observe hypotrabeculation, VSDs, rightward septal displacement, and RV hypoplasticity in *Tie2-Cre H2CKO* hearts. Occasionally (~20%), we observe a patent tricuspid valve that makes a direct connection with the LV, resulting in a double-inlet left ventricle (DILV), a CHD that functionally resembles TA (Figure 1J, arrow).

To examine atrioventricular (AV) cushion formation, cell density, and extracellular matrix (ECM) deposition, we stained sections with Alcian blue. Although comparison of *H2CKO* cushions with those of controls revealed no difference in size (Figures 1K and 1L), there appears to be a cushion-positioning defect (asterisk in Figure 1L). Despite normal AV cushion ECM deposition, no direct connection between the RA and RV is detected in any plane of section, resulting in a single left-sided AV canal in most *H2CKOs*, thus meeting the clinical definition of TA (Figure 1H). However, outflow tract (OFT) morphogenesis occurs normally in *H2CKOs* (Figures S1A–S1C).

While we also observe no defects in the yolk sac vasculature of *Tie2-Cre H2CKOs* (Figures S1D and S1E), Hand2 may play critical roles in vascular endothelium that could contribute to the observed embryonic lethality. Therefore, we used the endocardial-specific *Nfatc1^{Cre}* allele (Wu et al., 2012) to generate *H2CKOs* (Figures 1C, 1F, and 1N). This *Nfatc1^{Cre}* allele initiates expression throughout the endocardium at E9.0 (Wu et al., 2012), as opposed to the *Nfatc1^{enCre}* allele, which labels only a subset of valve endothelial cells. *Nfatc1^{Cre} H2CKOs* also show dramatic defects in trabeculation, malformed IVS, and atresia of the tricuspid valve (~70%; Figures 1F and 1N). Interestingly, in some cases, IVS malformations include large protrusions of myocardium that appear to indicate the formation of multiple IVSs (Figure 1N, arrows; Table S2). Robust expression of the septal/compact zone marker *Hey2* and the septal marker *Irx2* in these large protrusions confirm this observation, while expression of the trabecular marker Anf is excluded (Figures S2A–S2H). However, expression of the LV marker *Hand1* is not observed beyond the leftmost septum (Figures S2I and S2J). Tbx5, which has been suggested to induce the IVS (Takeuchi et al., 2003), is also unchanged (Figures S2K and S2L). Together, these data confirm that conditional deletion of *Hand2* within the endocardium is critical for normal trabeculation and septation. Given that these phenotypes are myocardial in nature, this suggests that endocardial Hand2 plays a crucial role in endocardium-to-myocardium signaling.

Hand2 Regulates *Nrg1* Expression within the Endocardium

We next investigated changes in gene expression within E10.5 *Tie2-Cre H2CKOs* using ISH. Expression analysis of *Fog2* was of interest, as *Fog2*-deficient mice also display TA (Svensson et al., 2000); however, no change in *Fog2* expression was observed (Figures S3A and S3B). Deletion of *Tgfbr2* from the endothelium results in DILV (Jiao et al., 2006). Analysis of *Tgfbr2* expression revealed no differences between *H2CKO* and controls (Figures S3C and S3D).

It has been directly demonstrated that endocardial Notch signaling plays an essential role in orchestrating morphogenic changes within the underlying myocardium, particularly during the process of trabeculation (Grego-Bessa et al., 2007). Therefore, we examined Notch pathway gene expression. We first analyzed expression of the Notch-regulated bHLH transcriptional repressors and potential Hand2 dimer partners, *Hey1* and *Hey2* (Figures S3E–S3H). Endocardial expression is not significantly changed. Next, we examined expression of the direct Notch1 target *EphrinB2* (*EfnB2;* Grego-Bessa et al., 2007). *EfnB2* ISH also shows no change in expression between *H2CKOs* and control embryos (Figures 2A–2D). However, epidermal growth factor family member *Neuregulin1* (*Nrg1*) is markedly downregulated at E10.5 within the endocardium of *H2CKOs* (Figure 2F, arrow in Figure 2H) compared to control embryos (Figure 2E, arrow in Figure 2G). *Nrg1* is known to be an essential mediator of trabeculation in the developing ventricles and is downregulated in *Tie2-Cre Notch1*CKOs, and *EfnB2* systemic null embryos (Grego-Bessa et al., 2007). The maintenance of *EfnB2* and loss of *Nrg1* in *H2CKOs* suggests that Hand2 acts downstream of *EfnB2*, but upstream of *Nrg1*, representing a novel step in *Notch1* trabeculation and septation signaling.

We next analyzed *Bmp10* expression, as myocardially expressed Bmp10 is crucial for proper trabeculation and is independently downstream of Notch1 signaling (Chen et al., 2004; Grego-Bessa et al., 2007). *BMP10* ISH at E10.5 suggests a subtle downregulation in *H2CKOs* (Figures S3I and S3J) while E12.5 ISH shows a near complete loss of *Bmp10*-expressing trabecular tissue within the RV but not LV (Figures 2I and 2J, arrows).

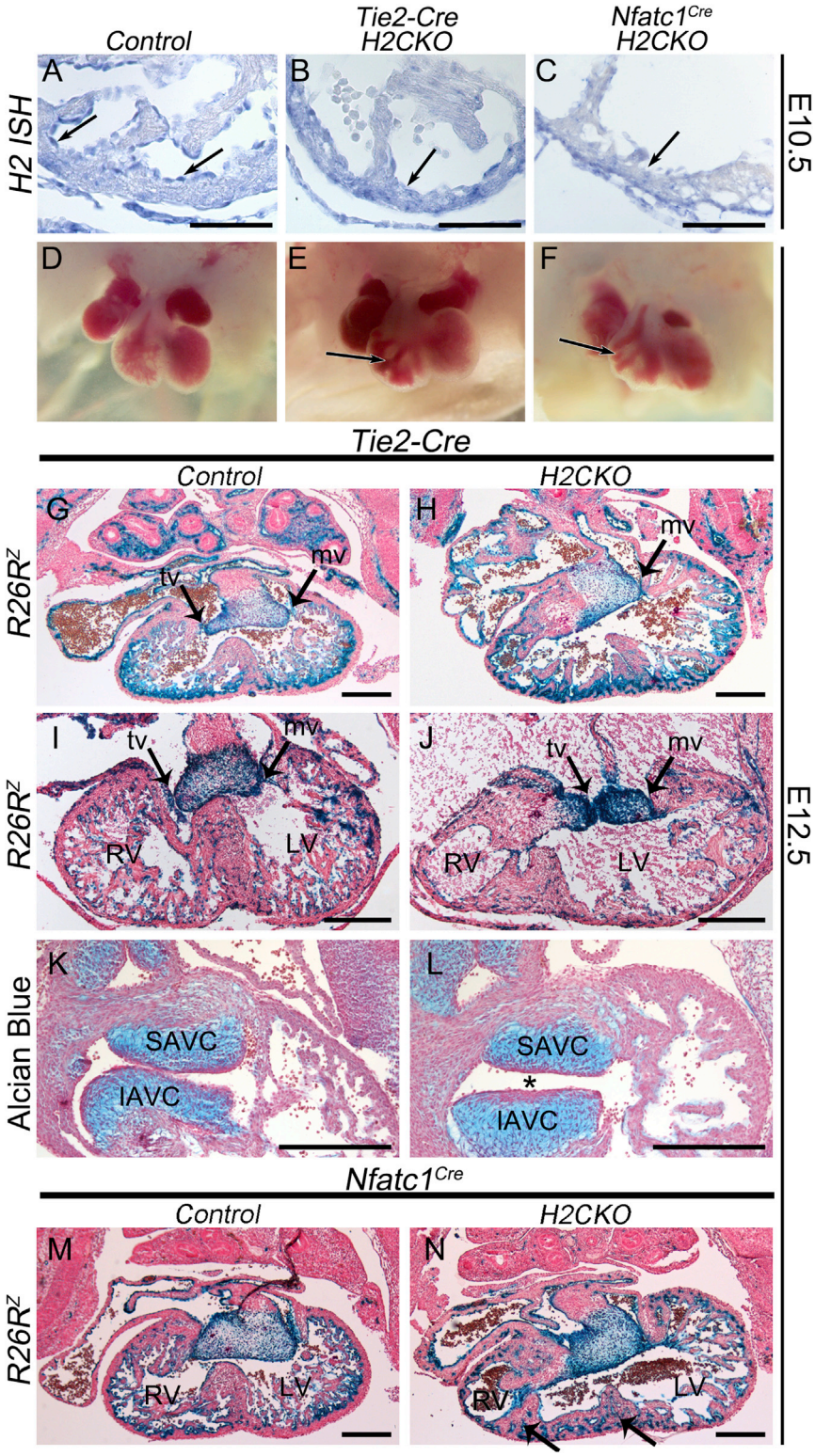

Figure 1. Endocardial Deletion of *Hand2* Results in a VSD, Hypotrabeculation, Hypoplastic RV, IVS Defects, and TA

(A–C) *Hand2 ISH* of RV sections from E10.5 control, *Tie2-Cre H2CKO,* and *Nfatc1^{Cre} H2CKO*, respectively.

(D–F) Whole-mount view of E12.5 control heart, *Tie2-Cre H2CKO*, and *Nfatc1^{Cre} H2CKO*, respectively.

(G and H) *R26R^{lacZ}*-stained sections from E12.5 *Tie2-Cre(+)* control embryo (G) and *Tie2-Cre H2CKO* with TA (H).

(I and J) *R26R^{lacZ}*-stained E12.5 *Tie2-Cre(+)* control embryo (I) and *Tie2-Cre H2CKO* with DILV (J).

(K–N) *R26R^{lacZ}*-stained sections from E12.5 *Nfatc1^{Cre}* control embryo (M) and *Nfatc1^{Cre} H2CKO* (N; arrows denote multiple IVSs). Alcian blue staining of E12.5 *Tie2-Cre(+)* control AV cushions (K) and *Tie2-Cre H2CKO* (L). Asterisk denotes abnormalities in AV cushion shape and position.

SAVC, superior atrioventricular cushion; IAVC, inferior atrioventricular cushion; tv, tricuspid valve; mv, mitral valve. Scale bars represent 100 μm in in (A)–(C) and 250 μm in in (G)–(N).

To quantitatively assess *Bmp10* expression, we dissected ventricles from E10.5 hearts and isolated RNA for quantitative RT-PCR (qRT-PCR). As expected, qRT-PCR analysis confirms that both *Hand2* and *Nrg1* are significantly downregulated in *H2CKOs* (Figure 2K) but *Bmp10* myocardial expression is not altered (Figure 2K). Thus, the reduction of *Bmp10* within the RV of E12.5 *H2CKOs* reflects the absence of RV trabeculation, as LV trabeculae express *Bmp10* (Figure 2J).

Endocardial Hand2 Functions Downstream of Notch1 and the Direct Notch1 Target EfnB2

Upon interaction with one of its transmembrane ligands, the transmembrane receptor Notch1 is proteolytically cleaved to generate the Notch1 intracellular domain (N1ICD). N1ICD translocates to the nucleus, where it dimerizes with its partner RBPJk to activate transcription of target genes. Previous studies have shown that deletion of *Notch1* or *RBPJk* results in hypotrabeculation due to loss of *EfnB2* and *Nrg1* (Grego-Bessa et al., 2007). To confirm that *Hand2* lies within the *Notch1* signaling pathway, we assayed *Hand2* expression in E9.5 *RBPJk*$^{-/-}$ embryos. Whole mount analyses reveal a loss of endocardial *Hand2*, while expression within the OFT and pharyngeal mesenchyme is unaffected (Figures 3A and 3B). Sectioned embryos confirm a specific loss of *Hand2* within mutant endocardium (Figures 3C and 3D), definitively establishing Hand2 as a Notch1 signaling effector.

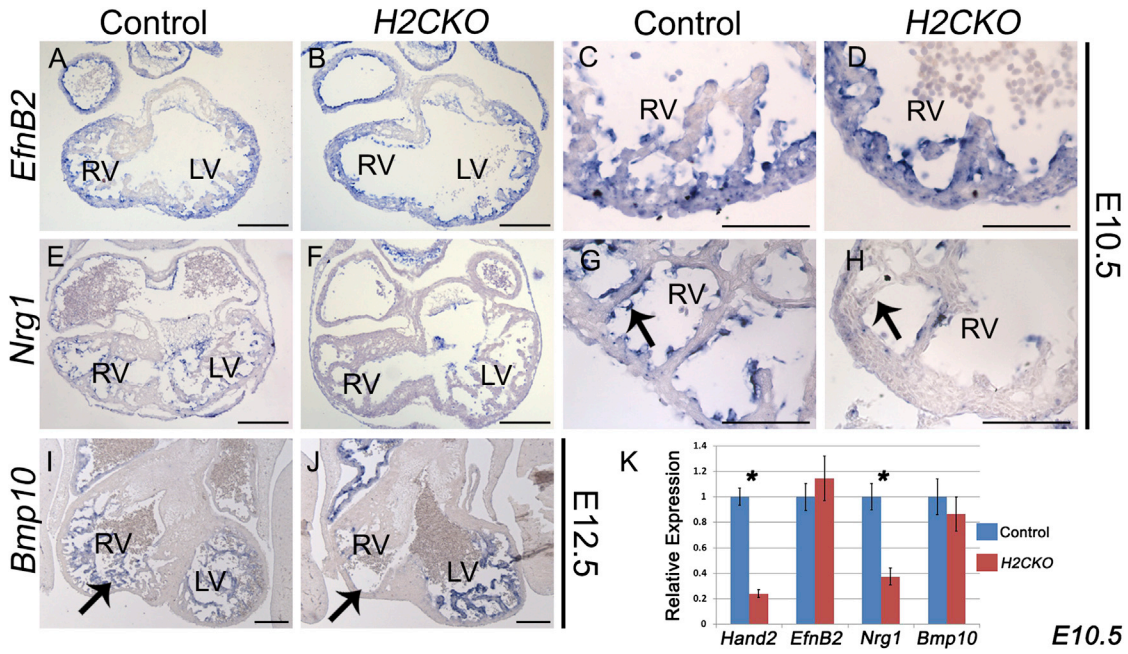

Figure 2. *H2CKOs* Exhibit Downregulation of *Nrg1* and Loss of *Bmp10*-Expressing Trabecular Myocardium

(A–D) Expression of the Notch1 target *EfnB2* is comparable between *H2CKOs* at E10.5 with controls.

(E–H) *Nrg1* expression at E10.5 is markedly decreased in *H2CKOs* when compared to controls (E–H; arrows in G and H denote endocardium).

(I and J) *H2CKOs* have less *Bmp10*-expressing trabecular myocardium in the RV at E12.5 (arrows denote trabecular tissue).

(K) qRT-PCR on isolated ventricles confirms the significant reduction (*$p \leq 0.05$) of *Nrg1* in E10.5 *H2CKOs*.

Scale bars represent 200 μm in (A), (B), (E), (F), (I), and (J) and 100 μm in (C), (D), (G), and (H).

During trabeculation, N1ICD/RBPJk directly transactivates *EfnB2*, which acts through its EphB2/EphB4 tyrosine kinase receptors to upregulate *Nrg1* (Grego-Bessa et al., 2007). While our data clearly show *Hand2* to be upstream of *Nrg1*, it was not clear if *Hand2* lies downstream of *EphrinB2* signaling or if *Hand2* represents a parallel *EfnB2*-independent Notch signaling pathway. To address this question, we assayed *Hand2* expression in E9.5 *Tie2-Cre(+);EfnB2*$^{fx/fx}$ embryos (Gerety and Anderson, 2002). ISH reveals that *Hand2* is downregulated in endocardial cells of *Tie2-Cre(+);EfnB2*$^{fx/fx}$ embryos (Figure 3F, arrow), whereas Hand2 expression in pharyngeal mesenchyme and the proepicardial organ is unaffected when compared to control hearts (Figure 3E). qRT-PCR analysis at E10.5 confirms *Hand2* downregulation within *Tie2-Cre(+);EfnB2*$^{fx/fx}$-isolated ventricles (Figure 3G). Together, these data show that Hand2 is a Notch-dependent endocardial factor positioned between *EfnB2* and *Nrg1*.

Hand2 Regulation of *Nrg1* Is Direct via Interaction with the *Nrg1* Promoter and Upstream Enhancer Sequences

As *Hand2* encodes a transcription factor with a similar expression profile to *Nrg1*, we sought to determine if Hand2 regulation of *Nrg1* is direct. An 850 bp region of the *Nrg1* promoter has been identified as necessary for high *Nrg1* transcriptional activity in vitro (Frensing et al., 2008). As Hand2 binds the consensus sequence CANNTG, termed an E-box, or alternatively CGNNTG, a D-box (Firulli et al., 2007), we searched this aligned promoter region for these conserved *cis* elements. Three were found within the 500 bp directly upstream of the *Nrg1* translation start site (Figure 4A). To assess Hand2 interaction with this region of the *Nrg1* promoter, we conducted chromatin immunoprecipitation (ChIP) assays in HeLa cells, employing a Myc-tagged Hand2 co-transfected with a plasmid encoding an untagged Hand2 dimerization partner, E12. Negative controls included Myc-Hand2 + E12 immunoprecipitated without αMyc, and *pCS2+Myc* samples immunoprecipitated with αMyc. Enrichment of the *Nrg1* promoter region was assessed by PCR using primers corresponding to a 103 bp region of the human *Nrg1* promoter. This amplicon shows robust enrichment within Myc-Hand2 + E12 immunoprecipitated samples (Figure 4B). To confirm that Hand2-E12 heterodimers are capable of binding the conserved consensus E/D-box sequences, double-stranded oligos corresponding to these sites were used in electrophoretic mobility shift assays (EMSA) with in vitro-translated Hand2 and E12 (Figure 4C). Hand2-E12 heterodimers specifically bind oligos corresponding to sites 1 and 3 (Figures 4D and 4E). No DNA binding is observed between Hand2-E12 complexes and site 2. To test if Hand2 is capable of transactivating the *Nrg1* promoter, *Hand2* and *E12* expression constructs were transfected into HeLa cells along with a *Nrg1* luciferase reporter containing the 1,000 bp directly upstream of the murine *Nrg1* translation start site. This region contains multiple transcription start sites located between −395 and −425 (Frensing et al., 2008). Co-transfection of *Hand2* and *E12* resulted in 7-fold reporter activation. Subsequent assays utilizing truncated promoters (−500/0 bp and −500/−250 bp) demonstrated more robust activation

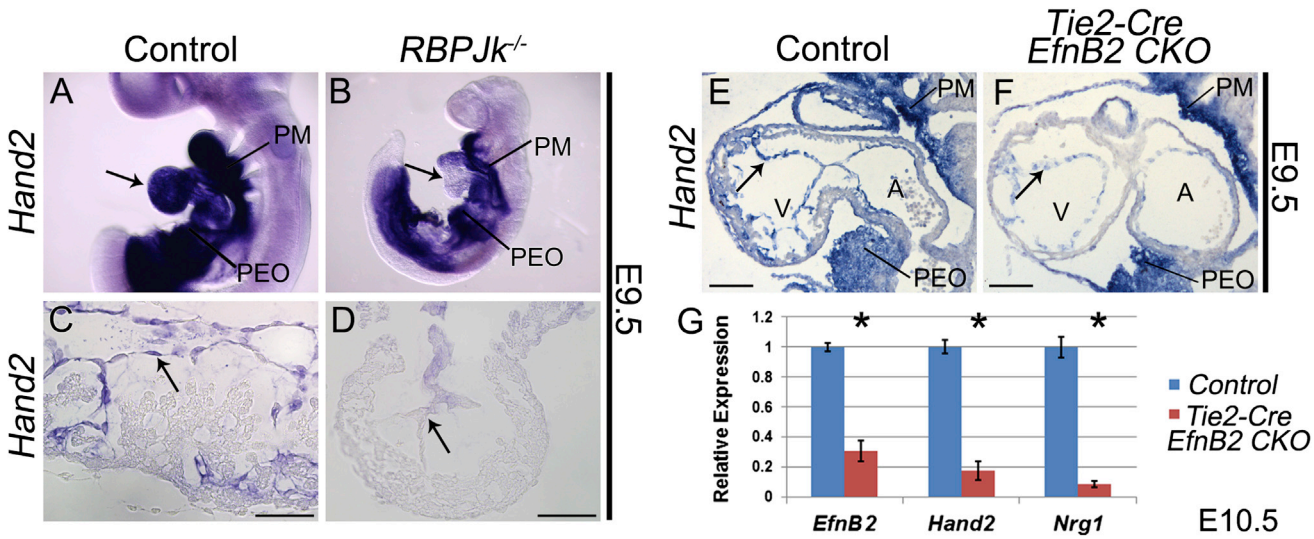

Figure 3. Hand2 Functions Downstream of Notch1 and the Direct Notch1 Target EphrinB2 during Trabeculation

(A and B) Whole-mount *Hand2* ISH in wild-type (A) and *RBPJk* knockout embryos (B). Arrows indicate endocardial *Hand2* expression in control (A) and loss of expression in *RBPJk* knockouts (B).

(C and D) *Hand2* ISH (C) shows robust endocardial Hand2 expression that is downregulated within RBPJk$^{-/-}$ endocardium (D).

(E and F) *Hand2* ISH (E) revealed a similar downregulation of *Hand2* within the endocardium of *Tie2-Cre EfnB2CKO* hearts (F; arrows denote endocardium).

(G) qRT-PCR on RNA isolated from ventricles confirms significant (*$p \leq 0.05$) downregulation of *Hand2* and *Nrg1* in *Tie2-Cre EfnB2CKO* hearts.

PM, pharyngeal mesenchyme; PEO, proepicardial organ. Scale bars represent 50 μm in (C) and (D) and 100 μm in (E) and (F).

(~18- and 16-fold, respectively; Figure 4F). Transactivation data from the 500 bp promoter revealed that E12 alone is not sufficient for activation, while Hand2 alone results in only modest (but significant) 3.5-fold transactivation. Consistent with EMSA results, cotransfection of Hand2 and E12 results in 18-fold transactivation, while a DNA-binding-deficient *Hand2* construct (Hand2Δbasic) is incapable of *Nrg1* transactivation alone or when cotransfected with E12 (Figure 4G).

Replacement of *Hand2* within *EfnB2*-Deficient Endocardium Results in an Improvement of Cardiac Trabeculation

EfnB2 mutant embryos display hypotrabeculation accompanied by loss of *Hand2* and *Nrg1* expression (Figure 4). Therefore, if Hand2 is both necessary and sufficient for regulation of *Nrg1*, we reasoned that *Hand2* replacement in *Nfatc1^{Cre} EfnB2CKOs* would restore *Nrg1* expression and improve ventricular trabeculation. To test this, we generated the Cre-activatable *Hand2* transgene *CAG-CAT-Hand2* (*CC-H2*; Figure S4A). Ectopic expression of Hand2 in limb mesenchyme results in preaxial polydactyly (McFadden et al., 2002). As predicted, *Prx1-Cre*-mediated activation of *CC-H2* within the limb results in polydactyly, indicating that the conditional transgene can be efficiently and specifically activated (Figure S4B). Similarly, *Nfatc1^{Cre}* efficiently activates *CC-H2* in the endocardium (Figure S4C). E13.5 *Nfatc1^{Cre}; CC-H2(+)* embryos do not display any obvious cardiac phenotypes (data not shown). Subsequently, *CC-H2(+); EfnB2$^{fx/+}$* females were then crossed with *Nfatc1^{Cre}; EfnB2$^{fx/+}$* males to generate *Nfatc1^{Cre}; CC-H2(+); EfnB2 CKOs*. *CC-H2(–); EfnB2 CKOs* die by E11.5, with severe pericardial edema, hemorrhaging, and defects in cardiac looping and chamber development (Figure 5C). These phenotypes closely resemble the defects observed in *Tie2-Cre EfnB2 CKOs* (Gerety and Anderson, 2002), indicating that while EfnB2 function within extracardiac vasculature is likely important, loss of endocardial *EfnB2* is sufficient to cause midgestation lethality. *Hand2* ISH at E10.5 confirms robust endocardial *Hand2* expression in controls (Figures 5E and 5F) and loss of *Hand2* in *EfnB2 CKOs* (Figure 5G, arrow). The presence of the *CC-H2* allele restores *Hand2* expression within the *EfnB2 CKOs* (Figure 5H, arrow; n = 3). *Nrg1* ISH reveals robust expression in controls (Figures 5I and 5J), and loss of *Nrg1* expression in *EfnB2 CKOs* (Figure 5K, arrow). *CC-H2(+); EfnB2 CKOs* display a significant increase in *Nrg1* expression (Figure 5L, arrow), while assessment of trabeculation by *Bmp10* ISH reveals a marked improvement in *Bmp10*-expressing trabecular myocardium (Figure 5P, arrow) when compared to *EfnB2 CKOs* lacking the *CC-H2* allele (Figure 5O, arrow). Expression analysis of isolated E10.5 ventricles by qRT-PCR demonstrates that while still well below control levels, *Nrg1* expression in *EfnB2* mutants that carry the *CC-H2* allele (n = 4) is twice as high as in *EfnB2* mutants lacking the *CC-H2* allele (upregulated 112%). *Bmp10* expression is increased by 79% with obvious improvement in trabeculation (Figure 5Q).

Notch-Dependent Hand2 Function Also Regulates Coronary Angiogenesis

The above analyses demonstrate that endocardial Hand2 plays a crucial role in myocardial morphogenesis. Myocardial trabeculation and compaction are intimately linked to endothelial cell behavior during development of the coronary vasculature by a complex signaling network that includes Vegf, Fgf, Tgf-β, and Notch components (Smart et al., 2009). Furthermore, early

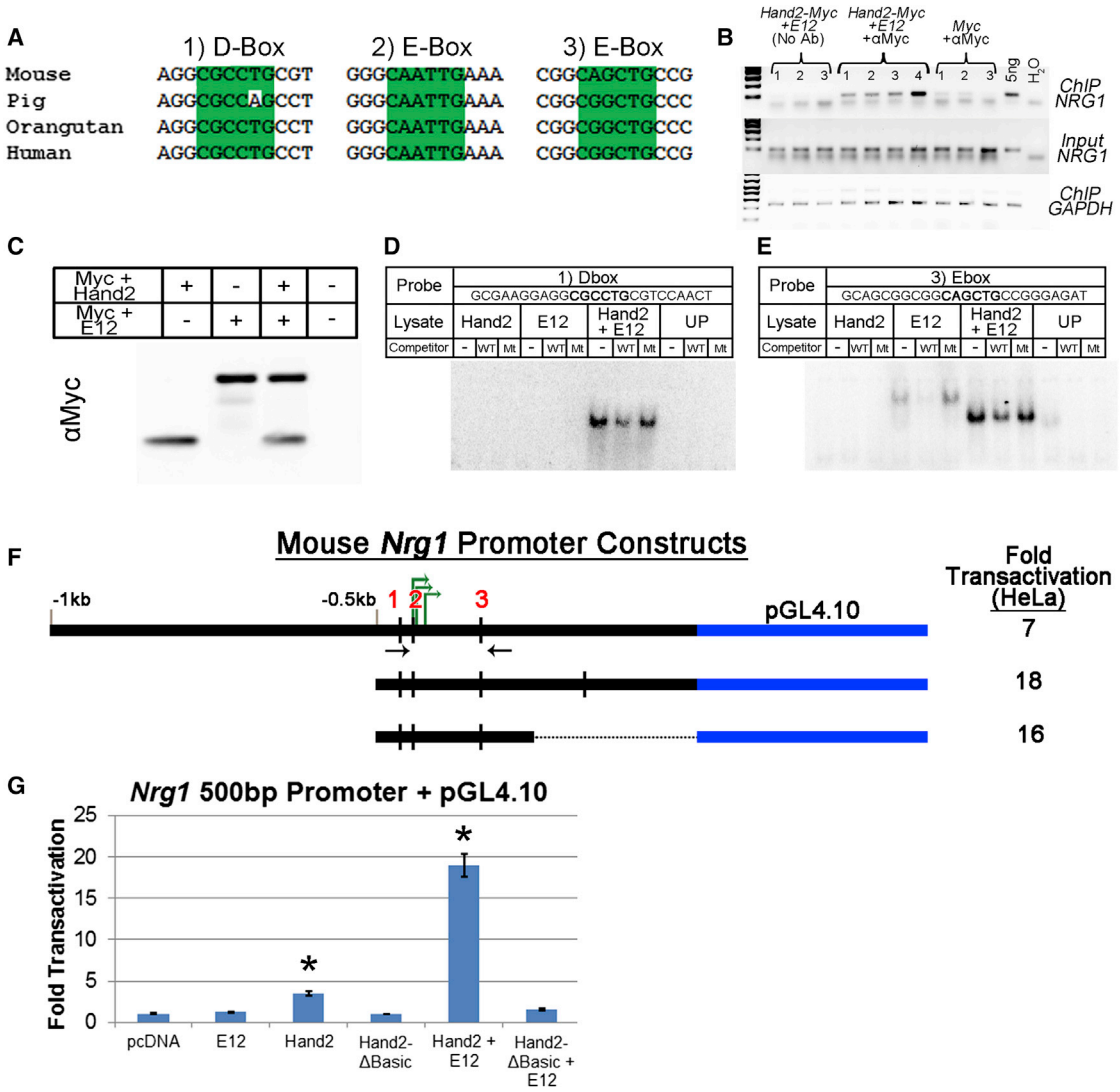

Figure 4. Hand2 Directly Regulates *Nrg1*

(A) Sequence alignments reveal three Hand2 consensus sites that are highly conserved among mammals.

(B) ChIP of the *NRG1* promoter.

(C) In vitro-transcribed and translated Hand2 and E12 used in EMSAs.

(D and E) EMSAs for D-box 1 (D) and E-box 3 (E) show robust and specific binding of Hand2-E12 heterodimers. No binding is observed for site 2.

(F) Luciferase reporter assays with a deletion series of the *Nrg1* promoter. Red numbers denote positions of the Hand2 consensus sites; green arrows denote positions of the transcription start sites; black arrows, location of ChIP primers.

(G) Transactivation of 500 bp *Nrg1* promoter reporter (*p $\leq$ 0.05).

embryonic lethality in genetic models of dysfunctional Notch signaling has precluded an in vivo assessment of the role of Notch signaling in formation of the coronary arteries. As we have established Hand2 as an integral component of endocardial Notch signaling, and as coronary endothelium is derived at least in part from the endocardium (Wu et al., 2012), the survival of *H2CKOs* to E14.5 allows us a unique opportunity to assess Notch function in early coronary development. Analysis of hearts at E13.5, 1 day after initiation of intramyocardial coronary formation (Tian et al., 2013), shows that *Nfatc1^{Cre} H2CKO* hearts (Figures 6B and 6D, arrows) exhibit an increased density of primitive coronary vessels when compared to control ventricles (Figures 6A and 6C). Subsequent analyses revealed a comparable degree of hypervascularization in *Tie2-Cre H2CKOs* (data not shown; Table S2). To ascertain the mechanism underlying this hypervascularization, we analyzed genes associated with vascular development in E10.5 and E13.5 *Nfatc1^{Cre} H2CKO* isolated ventricles by qRT-PCR (n = 4; Figures 6E and 6F, respectively). As expected, expression levels of *Hand2* and *Nrg1* are down at both time points. Analysis of vascular markers at E10.5 reveals dysregulation of select components of Vegf signaling (Figure 6E). *VegfR2* is downregulated by 30%, and its

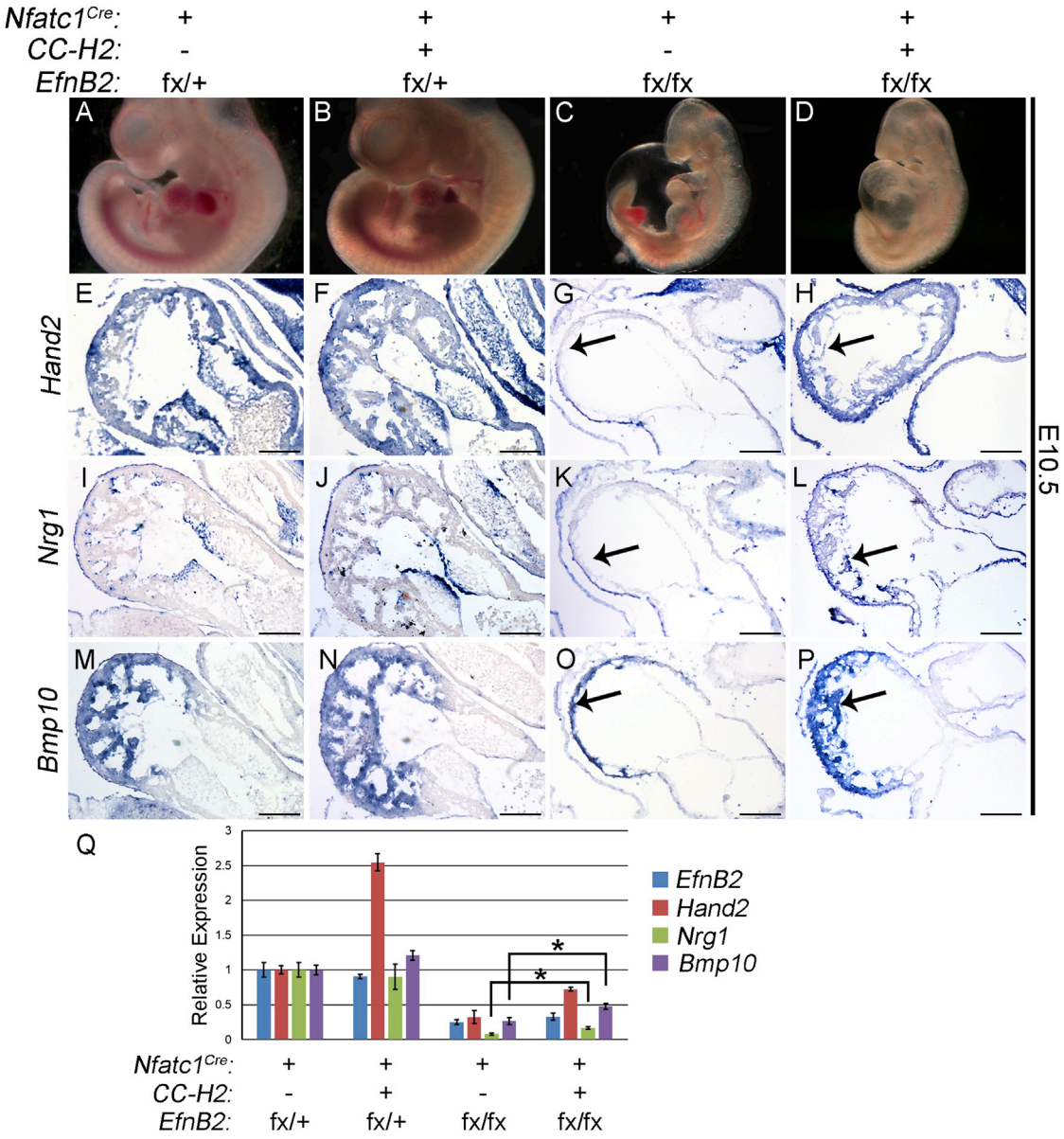

Figure 5. Conditional *CAG-CAT-Hand2* Transgene Expression in *Nfatc1*^{Cre} *EfnB2 CKOs* Partially Improves Trabeculation and *Nrg1* Expression

(A–D) Whole-mount images of E10.5 control, *CC-H2(+)* control, *EfnB2 CKO*, and *CC-H2(+)*; *EfnB2 CKO* embryos.

(E–H) *Hand2* section ISH. Arrow in (G) indicates loss of *Hand2*; arrow in (H) indicates restoration of endocardial Hand2 via *CC-H2*.

(I–L) *Nrg1* section ISH. Arrow in (K) indicates loss of *Nrg1 in EfnB2 CKOs*; arrow in (L) indicates restored *Nrg1* expression in *EfnB2 CKOs* that are also *CC-H2(+)*.

(M–P) *Bmp10* section ISH. Arrow in (O) indicates *Bmp10*-expressing myocardium and lack of trabeculation; arrow in (P) indicates restoration of *Bmp10*-expressing trabeculations.

(Q) qRT-PCR analysis of isolated E10.5 ventricles. Asterisks denote significant difference ($p \leq 0.05$). *CC-H2*, *CAG-CAT-Hand2*.

Scale bars in (E)–(P) represent 100 μm.

coreceptor *Nrp1* is downregulated by 14%. *VegfD*, which encodes a VegfR3-specific ligand, is downregulated by 25%. By E13.5, expression levels of *VegfR2* and *VegfD* have recovered (Figure 6F), whereas *Nrp1* remains downregulated. Surprisingly, expression of *VegfA*, which encodes the primary Vegf ligand that regulates vascular development (Ferrara et al., 1996), is upregulated by over 200%. Expression of *VegfR3* is upregulated by 120%, and expression of *Dll4*, which encodes a notch ligand regulated by VegfRs (Wythe et al., 2013), is upregulated by approximately 85%. Differential regulation of several additional key vascular factors was also observed at E13.5. The venous markers *CouptfII* and *EphB4* are downregulated by 21% and 24% respectively, while the arterial marker *EfnB2* is downregulated by 33%. Surprisingly, *Sox18* and *Lyve1*, which encode

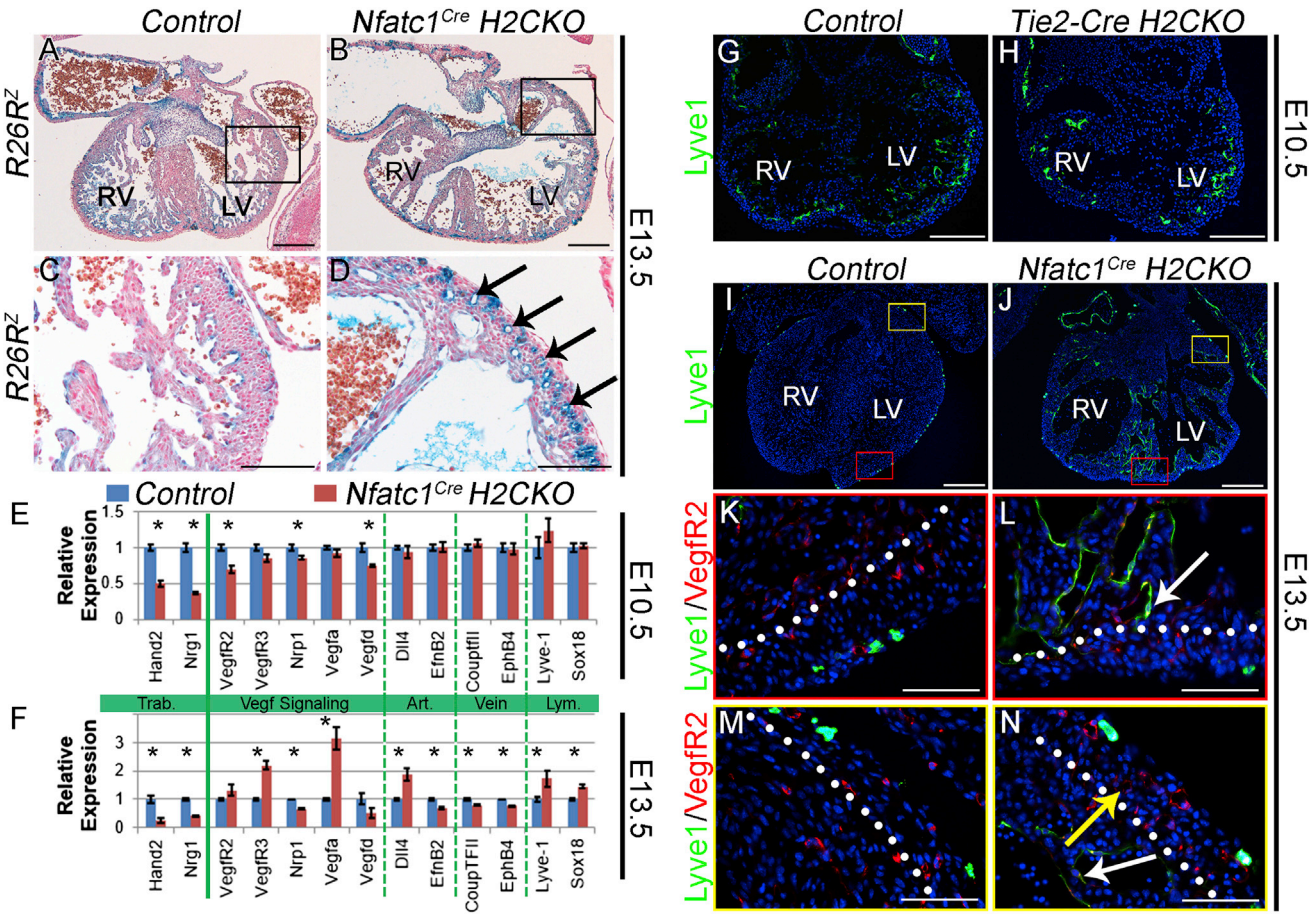

Figure 6. Hand2 Controls Coronary Development and Endocardial Maturation via Regulation of Vegf Signaling

(A and B) *R26R*^{lacZ}-stained E13.5 hearts.

(C and D) LV outer curvature. *Nfatc1*^{Cre} *H2CKOs* display hypervascularization (arrows in D).

(E and F) qRT-PCR analysis of E10.5 and E13.5 gene expression (n = 4) in *Nfatc1*^{Cre} *H2CKOs* (asterisks denote significant difference, $p \leq 0.05$).

(G and H) Lyve-1 immunostaining in E10.5 Control and *Tie2-Cre H2CKO* hearts.

(I–N) Lyve-1 immunostaining in E13.5 Control and *Nfatc1*^{Cre} *H2CKO* hearts. In E13.5 control hearts Lyve-1 expression is restricted to endothelial lymphatic precursors (K), while *H2CKOs* continue to express Lvye-1 within ventricular endocardium (L, white arrow). Persistent Lyve-1 expression marks ventricular endocardium (N, white arrow), but not coronary endothelium (N, yellow arrow). Dotted lines denote the border between compact and trabecular myocardium. Scale bars represent 250 μm in (A) and (B), 100 μm in (C) and (D), 200 μm in (G) and (H), 250 μm in (I) and (J), and 50 μm in (K)–(N).

factors typically associated with endothelium of the lymphatic system, were upregulated by 45% and 73% respectively. To determine what cardiac cell populations were upregulating Lyve-1, we conducted Lyve-1 immunostaining at E10.5 (Figures 6G and 6H) and E13.5 (Figures 6I–6N) in control and *H2CKO* hearts. Sections from E13.5 hearts were costained with VegfR2 to mark cardiac endothelium (see Table S3 for a glossary of terminology pertaining to endothelial cell populations). E10.5 immunostaining reveals that Lyve-1 is expressed robustly within endocardium of both control and *H2CKO* hearts. In contrast, by E13.5, Lyve-1 immunostaining in control hearts is restricted to a population of peripheral cardiac macrophages (Figure 6I; Pinto et al., 2012), whereas robust Lyve-1 immunostaining persists in the ventricular endocardium of *H2CKOs* (Figures 6J and 6L). However, while Lyve-1 still robustly marks *H2CKO* ventricular endocardium (Figure 6N, white arrow), Lyve-1 expression does not mark the expanded coronary endothelium of *H2CKOs* (Figure 6N, yellow arrow).

As previously mentioned, qRT-PCR demonstrates differential expression of several Vegf signaling components. We therefore investigated, using ChIP, ChIP sequencing (ChIP-seq), EMSA, and luciferase reporter assays, the possibility that Hand2 directly regulates at least a subset of these components (Figure 7A). Given that our results establish Hand2 as a downstream effector of Notch signaling, and Notch also regulates expression of *VegfRs* within endothelial cells (Herbert and Stainier, 2011), we first addressed the possibility that Hand2 directly regulates *VegfR3* expression. Using the previously described HeLa ChIP samples, we show that immunoprecipitation of *Hand2-Myc/E12*-transfected cell lysates results in selective enrichment of a region within the *VegfR3* promoter that has been previously reported to have regulatory activity (Figure 7B; Shawber et al.,

A

	Expression in E13.5 *H2CKOs*	Detected by Hand2 ChIP-Seq	Luciferase Reporter Transactivation
VegR3	↑ 120%	No	50% repression
Nrp1	↓ 35%	Yes	5 fold activation
Vegfa	↑ 215%	No	N/A
Dll4	↑ 85%	Yes	No repression

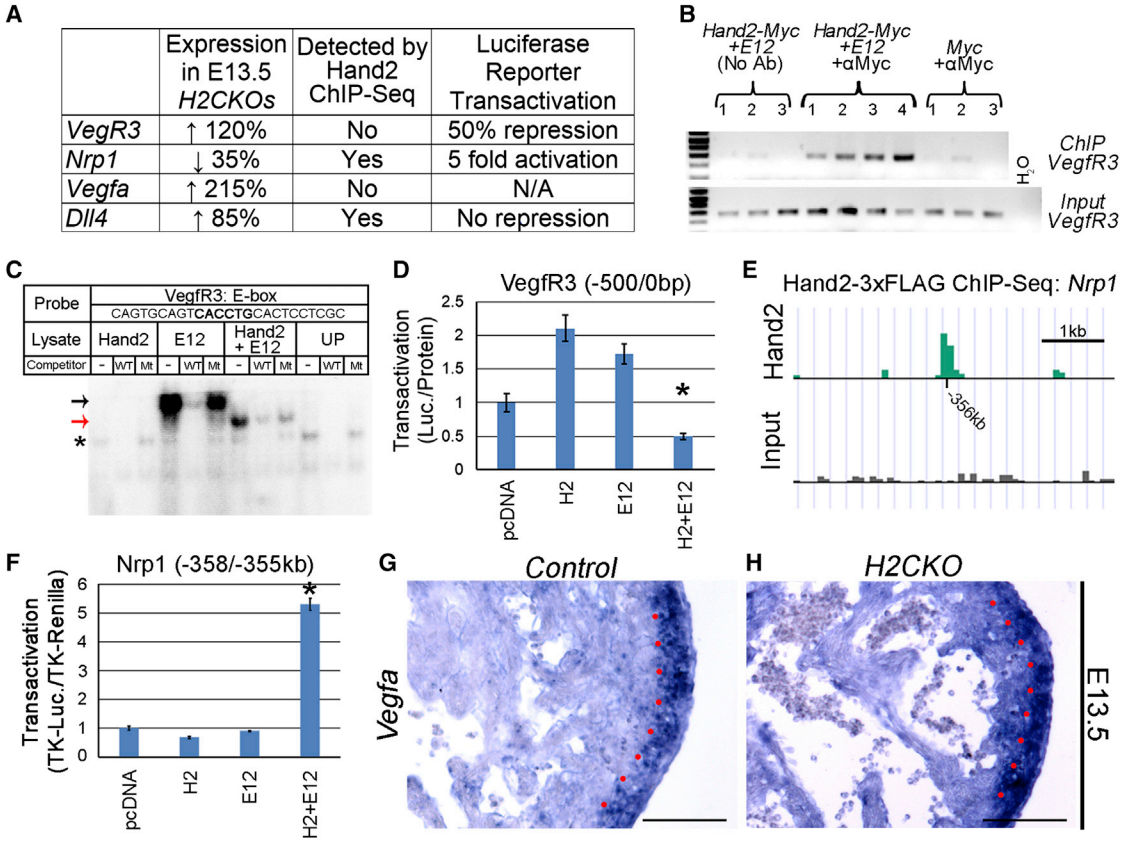

Figure 7. Hand2 Regulates Vegf Signaling

(A) Differentially expressed genes that were analyzed for direct regulation by Hand2.

(B) ChIP of a region within the 500 bp *VegfR3* promoter.

(C) EMSA demonstrates Hand2-E12 heterodimers specifically bind an oligo corresponding to an E-box within the ChIP amplicon of the *VegfR3* promoter. Black arrow indicates E12 homodimer binding, red arrow indicates Hand2-E12 heterodimer binding, and asterisk indicates nonspecific binding.

(D) Hand2-E12 heterodimers repress significantly ($p \leq 0.05$) a luciferase reporter containing the 500 bp *VegfR3* promoter.

(E) *Hand2-3xFLAG* ChIP-seq demonstrates a prominent region of enrichment approximately 356 kb upstream of the *Nrp1* coding region.

(F) A luciferase reporter containing this potential enhancer region is significantly ($p \leq 0.05$) transactivated 5-fold by H2-E12 heterodimers.

(G) ISH demonstrates strong myocardial expression of *VegfA* within the compact zone of control E13.5 hearts. Red dots denote the border between compact and trabecular myocardium.

(H) In *H2CKOs*, the distinction between *VegfA* expression levels in compact versus trabecular myocardium is more poorly defined.

Scale bars in (G) and (H) represent 100 μm.

2007). Furthermore, by EMSA, we show that Hand2 E12 heterodimers specifically bind an oligo corresponding to one of the two E-boxes within this human promoter region (Figure 7C), which consists of the 500 bp upstream of the *VegfR3* translation start site. Finally, a luciferase reporter containing the homologous 500 bp mouse promoter was significantly repressed by Hand2 E12 heterodimers (~50% repression; $p \leq 0.05$; Figure 7D). Collectively, these data indicate that Hand2 may directly repress *VegfR3* expression within cardiac endothelium.

To detect additional Hand2 targets, we utilized a Hand2 ChIP-seq data set that was generated for an alternate study (Osterwalder et al., 2014). This ChIP-seq data set employed a *Hand2-3xFLAG* knockin allele. E10.5 Hand2-expressing tissues, including the heart, were collected and used for an immunoprecipitation of Hand2-bound regions of genomic DNA. This data set was cross-referenced with our *H2CKO* gene expression data, where in addition to increased *VegfR3*, we observed decreased expression of the VegfR2 cofactor *Nrp1*. Analysis of *Hand2-3xFLAG* ChIP-seq data revealed a region of high enrichment 356 kb upstream of the *Nrp1* coding region (Figure 7E; Table S4). An approximately 3 kb region containing this potential enhancer was cloned upstream of a luciferase reporter driven by the thymidine kinase (TK) minimal promoter. When cotransfected into HeLa cells with *Hand2* and *E12*, a significant 5.2-fold transactivation was observed (Figure 7F). Analysis of *VegfR3* and *Nrp1* expression by ISH reveals expression within cardiac endothelium (Figures S5A and S5B), although differential expression between controls and *H2CKOs* is not detectable by this nonquantitative assay.

Given that *VegfA* is upregulated by over 200% in E13.5 *H2CKOs*, we analyzed the *Hand2-3xFLAG* ChIP-seq data set for evidence of direct regulation. No prominent peaks were

Please cite this article in press as: VanDusen et al., Hand2 Is an Essential Regulator for Two Notch-Dependent Functions within the Embryonic Endocardium, Cell Reports (2014), http://dx.doi.org/10.1016/j.celrep.2014.11.021

detected within the *VegfA* locus. Indeed, ISH demonstrates that *VegfA* expression is not detectable within endocardium. However, *VegfA* is strongly expressed within the myocardial compact zone, with low levels of expression observed within trabeculae (Figure 7G). In *H2CKOs*, the difference in expression levels between compact and trabecular myocardium is visibly less distinct, with high *VegfA* expressing regions appearing to extend beyond the compact zone (Figure 7H).

DISCUSSION

Loss of *Hand2* within the SHF cardiac progenitors that give rise to both endocardial and myocardial lineages has been associated with TA. In this study, we show that loss of *Hand2* specifically in the endocardium, a cell population in which robust *Hand2* expression has previously gone uninvestigated, can cell-autonomously generate TA. These results underscore the importance of effective endocardial-myocardial signaling during early cardiac morphogenesis. Mechanistically, our data show that endocardial Hand2 sits downstream of Notch1 and EfnB2 and is itself directly upstream of *Nrg1,* being necessary and sufficient for *Nrg1* expression in vivo. Notch signaling is a well-established component of endocardium-to-myocardium communication. Hand2 endocardial roles include regulation of trabeculation, positioning of the IVS, and IVS morphogenesis. Indeed, endocardial *H2CKOs* present multiple septa that are marked by *Irx2* and compact zone/septal marker *Hey2*, while excluding trabecular marker *Anf* (Figure S2). These ectopic right-sided septa do not express *Hand1* or *Tbx5* at their left side base (Figures S2I–S2L), suggesting that these septa form via a noncanonical mechanism from RV cardiomyocytes.

These data demonstrate that endocardial Hand2 regulates the specification of trabecular and septal myocardium from primitive myocardium. Given the striking similarities between the cardiac defects of *EfnB2* knockouts (Figures 3F and 3G), which do not express *Nrg1*, and the reported phenotypes of *Nrg1* knockouts (Kramer et al., 1996), the most logical conclusion is that loss of *Nrg1* expression is the root cause of the hypotrabeculation, septal, and TA phenotypes observed in *H2CKOs*.

We show that trabeculation and *Nrg1* expression within *EfnB2* CKO mice is improved by *Hand2* replacement via the *CC-H2* transgene (Figure 5). Hand2 is necessary for normal expression of *Nrg1* (Figure 2), and we demonstrate that Hand2 is sufficient for partial restoration of *Nrg1* expression levels in *EfnB2 CKOs*. While trabeculation is markedly improved in *CC-H2(+) EfnB2 CKOs*, these embryos still display hallmarks of cardiovascular failure such as pericardial edema and hemorrhage. The incomplete restoration of normal cardiac phenotype is not surprising given that restoration of *Nrg1* expression is incomplete, and EfnB2 signaling likely has a much broader range of endocardial downstream targets then just *Hand2*. Our observation that ~37% of *Nrg1* expression remains in *Tie2-Cre H2CKOs* (Figure 2K) while less than 10% remains in *Tie2-Cre EfnB2 CKOs* (Figure 3G) indicates that EfnB2 also influences *Nrg1* expression via Hand2-independent inputs.

While it is clear that endocardial loss of *Hand2* impairs the Notch-dependent processes of trabeculation and septal development, it is less clear how this impairment results in TA. It is possible that multiple morphogenic inputs contribute to the TA observed in *H2CKOs*. Previous studies have concluded that TA occurs when the atrial connection to the AV canal expands rightward but the ventricular inner curvature fails to remodel (Kim et al., 2001). Given the dramatic myocardial defects observed in *H2CKOs*, Hand2-dependent remodeling of AV canal myocardium could be involved; however, histological analysis of *H2CKOs* suggests a simpler model wherein the septum shifts rightward in *H2CKOs* and interferes with development of the primitive right AV canal, thus resulting in TA. Indeed, we show that *Tie2-Cre H2CKOs* have a smaller RV, which is not due to increased cell death within SHF progenitors, increased cell death within the RV, or decreased proliferation within the RV (Figures S6A–S6D). Furthermore, analysis of ventricle areas reveals that *Tie2-Cre H2CKOs* have a smaller RV and larger LV but no change in total area (Figure S6E), thus supporting histological observations of a rightward-shifted septum. In extreme rightward septal shifts, AV cushion maturation is not hindered but the tricuspid valve forms above the LV, thus resulting in DILV. Finally, *Hand2* ablation within the developing OFT and AV valve mesenchyme does not alter septation or valve morphogenesis and does not result in TA (VanDusen et al., 2014). In total, these data demonstrate a cell-autonomous Hand2-dependent role of the endocardium in the etiology of TA/DILV.

In addition to the dramatic defects in myocardial morphogenesis observed in endocardial *H2CKOs*, histological analyses at E13.5 also reveal significant vascular phenotypes. *H2CKOs* display precocious and disorganized development of the coronary vascular plexus. Analysis of vascular related gene expression in E10.5 and E13.5 *H2CKOs* surprisingly reveals that major components of cardiac Vegf signaling are dysregulated. *VegfR2* and *VegfD* are downregulated at E10.5, while *VegfR3* and *VegfA* are significantly upregulated by E13.5. Additionally, VegfR2 coreceptor *Nrp1* is downregulated at both E10.5 and E13.5, while expression of the notch ligand *Dll4* is increased at E13.5, an indication of enhanced Vegf signaling (Figures 6E and 6F). Furthermore, qRT-PCR and immunostaining reveals elevated expression of the receptor Lyve-1 within endocardium of E13.5 *H2CKOs*. Analysis at E10.5 demonstrates that Lyve-1 is initially expressed throughout the early endocardium and is subsequently downregulated as the endocardium matures, such that by E13.5, expression is no longer detectable within ventricular endocardium but is observed only within cardiac macrophages. Given the early endocardial expression of Lyve-1, this persistence within *H2CKOs* most likely represents a defect in endocardial maturation, rather than ectopic activation of the lymphatic gene program.

Of the genes we observed to be differentially expressed in E13.5 *H2CKOs*, both the *Dll4* and *Nrp1* loci contain prominent Hand2 Chip-seq peaks (Table S4). *Nrp1* encodes an isoform-specific VegfA receptor that acts in concert with VegfR2. Interestingly, an RNA subtractive hybridization screen previously identified *Nrp1* as being downregulated in Hand2 systemic null embryos (Yamagishi et al., 2000). Our data indicate that *Nrp1* is an endocardial target of Hand2, although regulation may also occur in additional tissues where these factors are coexpressed (Figure S5A). Cotransfection of *Hand2* and *E12* with a luciferase reporter containing the potential upstream

enhancer region yielded over 5-fold transactivation, further supporting direct regulation of *Nrp1* by Hand2. In contrast, luciferase reporter assays failed to demonstrate Hand2-mediated repression via the enriched Dll4 upstream region, indicating that the increased Dll4 expression in *H2CKOs* may be secondary to changes in expression of Vegf receptors, which are known to regulate Dll4 (Wythe et al., 2013). However, our data do not rule out Hand2 direct regulation of *Dll4* by alternate undetected enhancers. Expression of *VegfR3* is upregulated in E13.5 *H2CKOs* by over 100%. VegfR3 is capable of functioning as both a homodimer and VegfR3-VegfR2 heterodimer, and distinct functions have been associated with different interactions (Dixelius et al., 2003). VegfR3 plays crucial roles in angiogenic sprouting and development of the lymphatic system (Benedito et al., 2012), and we show that *VegfR3* is expressed within at least a subset of the endocardium (Figure S5B, arrow). While no high-ranking ChIP-seq peaks were observed within the *VegfR3* locus, cardiac endothelium represents only a small portion of the total *Hand2* expressing tissue that was utilized, and so sensitivity may be a limiting factor of this assay. Our HeLa ChIP results indicate that Hand2 interacts with the *VegfR3* promoter, while transactivation assays correlate with *H2CKO* expression data, indicating that Hand2 may repress *VegfR3* transcription. In addition to *VegfR3*, we observe a 45% increase in *Sox18* expression at E13.5. As *Sox18* specifically marks endothelium of the coronary vasculature at this time point (Figure S5C), this increase most likely reflects the hypervascularization phenotype.

Similar to several extracardiac angiogenic models of Notch signaling obstruction (Benedito et al., 2012; Tammela et al., 2008), we show that endocardial *Hand2* ablation results in a hypervascularization phenotype featuring the formation of an excessive number of new vessels. Furthermore, we show that this phenotype is accompanied by broad dysregulation of Vegf signaling. Homeostasis of Vegf signaling is crucial during embryonic development, as mice heterozygous for a *VegfA* null mutation die at E9.5, while an increase in *VegfA* expression (~3-fold) results in lethality at approximately E13.5 (Miquerol et al., 2000). In the present study, we demonstrate that expression of *VegfA* is expanded in *H2CKOs*. This could reflect aberrant specification of trabecular myocardium or secondary pathological effects of compromised cardiac function. *VegfA* is the most differentially regulated gene that we observe, while *VegfR2*, *VegfR3*, and *Nrp1* are also dysregulated within *H2CKOs*. Given the complex interactions that take place between these molecules, disrupted receptor stoichiometry and upregulated *VegfA*, a growth factor that is well known for its proangiogenic qualities, most likely account for the observed coronary phenotype. These data not only provide insight into a second novel function of Hand2 within the endocardium but also reveal a wider role of Notch signaling during coronary vessel development. Coronary heart disease is a major cause of mortality in developed nations, being responsible for approximately one of every six deaths in the United States (Go et al., 2013). Consequently, further assessment of Hand2's regulatory role in Vegf signaling during coronary vascularization, as well as potential adult homeostatic roles of Hand2-dependent Notch signaling, is an interesting avenue of future investigations.

EXPERIMENTAL PROCEDURES

Mice and Genotyping

Tie2-Cre(+) and *Nfatc1-Cre(+)* mice were crossed with *Hand2*$^{+/-}$ mice to generate *Tie2-Cre(+);Hand2*$^{+/-}$ and *Nfatc1-Cre(+);Hand2*$^{+/-}$ males. These males were then crossed with *Hand2*$^{fx/fx}$*;ROSA26R* reporter mice (*lacZ* or *eYFP*) to generate conditional null *Hand2* embryos. *Tie2-Cre(+)* females were crossed with *EfnB2*$^{fx/fx}$ males to generate *Tie2-Cre(+);EfnB2*$^{fx/+}$ males. These males were then crossed with *EfnB2*$^{fx/fx}$ females to generate conditional null *EfnB2* embryos. The cre-activatable transgene *CAG-CAT-Hand2* was constructed by replacing the *Myc-Twist1* cDNA of *CAG-CAT-Twist* (Connerney et al., 2006) with the murine *Myc-Hand2* cDNA. This construct was used for microinjection to establish a transgenic line. For genotyping information, see Supplemental Experimental Procedures. Mouse maintenance and experimentation was performed according to protocols approved by the Indiana University School of Medicine Institutional Animal Care and Use Committee.

Hand2-3xFLAG ChIP-Seq

The Hand2 ChIP-seq data set was generated as part of a previous study using homozygous *Hand2-3xFLAG* embryos, which express a 3xFLAG epitope-tagged Hand2 protein (Osterwalder et al., 2014). Briefly, Hand2-expressing tissues (heart, limbs, and pharyngeal arches) from 150 *Hand2-3xFLAG* E10.5 embryos were dissected and pooled. Samples were crosslinked in 1% formaldehyde for 5 min and ChIP was performed using FLAG antibodies (Sigma F1804). ChIP-seq reads were mapped to the mouse genome (NCBI37/mm9) and peaks were detected using MACS (version 1.3.7.1) for the *HAND2-3xFLAG* and input control samples. Statistically validated peaks were sorted according to fold enrichment and number of reads.

Section RNA In Situ Hybridization

Antisense digoxigenin labeled riboprobes were transcribed with T7, SP6, or T3 (Roche). Section ISH was performed as previously described (Vincentz et al., 2008). The cDNA for a *Fog2* riboprobe was kindly supplied by Eric Svensson, *Tbx20* by Simon Conway, *Anf* and *Irx2* by Vincent Christoffels, *TgfβR2* by Henry Sucov, and *EfnB2* by Hai Wang. All data reflect assessment in $n \geq 3$ embryos for ISH and immunostaining and $n \geq 4$ for qRT-PCR analyses.

Quantitative RT-PCR

Total RNA was isolated from E10.5 or E13.5 ventricles using the High Pure RNA Isolation Kit (Roche). This RNA served as a template to generate cDNA using the Transcriptor First Strand cDNA Synthesis Kit (Roche). For qRT-PCR, cDNA was amplified using TaqMan Probe-Based Gene Expression Assays (Applied Biosystems). Relative gene expression was determined after normalization to GAPDH. The Student's t test was used to detect significant differences between sample groups; asterisks denote p values ≤ 0.05. Error bars represent SE.

EMSAs, Luciferase Assays, and ChIP

Hand2 and E12 were in vitro translated using the Promega Reticulocyte Lysate System. A total of 5 μl of translated protein was incubated in binding buffer for 30 min at 25°C with radiolabeled oligos corresponding to E-boxes and D-boxes within the *Nrg1* and *VegfR3* loci (Firulli et al., 2007). Transcription factor/oligo complexes were run out on a nondenaturing 6% polyacrylamide gel and assessed on a phosphoimager. For luciferase assays, HeLa cells were transfected using X-tremeGENE HP (Roche) at a ratio of 3:1 with *Nrg1-500bp+pGL4.10* (luciferase), *VegfR3-500bp+pGL4.10* (luciferase), *pGL4.73* (SV40-renilla) or *pGL4.74* (TK-renilla), *Pcs2+Myc-Hand2*, *Pcs2+Myc-E12*, *pcDNA*$^{+}$*Myc-ΔBasic-Hand2* (kindly provided by Eric Olson), or *pcDNA3.1* and cultured for 48 hr. After harvest and processing, luciferase and renilla reporter activity was assessed in equal amounts of cell lysate using Luminoskan Ascent software and a ThermoLabsystems luminometer. Luciferase results were normalized to protein concentration or renilla. Asterisks denote significant difference from *pcDNA* control (p value ≤ 0.05); error bars represent SE. For construction of Nrp1(−358/−355 kb) and Dll4(−23/−20 kb) luciferase reporters, genomic regions containing a *Hand2-3xFLAG* ChIP-seq peak were PCR amplified and cloned into *TK-pGL4.10*. For ChIP of the *Nrg1* promoter, HeLa cells were again transfected using X-tremeGENE HP at a ratio

Please cite this article in press as: VanDusen et al., Hand2 Is an Essential Regulator for Two Notch-Dependent Functions within the Embryonic Endocardium, Cell Reports (2014), http://dx.doi.org/10.1016/j.celrep.2014.11.021

of 3:1. After culturing for 48 hr, cells were processed as previously described (Barnes et al., 2011). Briefly, equal amounts of sheered chromatin were immunoprecipitated overnight at 4°C with 50 μl of αMyc-conjugated agarose beads (Sigma) or beads without antibody for a negative control. After reversing cross-links, eluted immunoprecipitated DNA was phenol chloroform extracted, re-suspended in ddH_2O, and used for subsequent PCR reactions. After 37 cycles of PCR amplification, product was analyzed on an agarose gel. ChIP transfection constructs included *Pcs2+Myc-Hand2*, *Pcs2+E12*, and *Pcs2+Myc*. See Supplemental Experimental Procedures for oligo information.

SUPPLEMENTAL INFORMATION

Supplemental Information includes Supplemental Experimental Procedures, six figures, and four tables and can be found with this article online at http://dx.doi.org/10.1016/j.celrep.2014.11.021.

AUTHOR CONTRIBUTIONS

N.J.V. wrote the manuscript, conceived of experiments, and carried out experiments. J.C. carried out experiments and critically read the manuscript. J.W.V. and B.A.F. interpreted data, provided reagents, and critically read the manuscript. R.Z., M.O., and J.L.R. conceived of and carried out *Hand2-3xFLAG* ChIP-seq. B.Z. aided in experimental planning and provided $Nfatc1^{Cre}$ mice. J.G.B. and J.L.P. assayed *Hand2* expression in $RBPJk^{-/-}$ mice. W.S. interpreted data and evaluated the manuscript. A.B.F. wrote and edited the manuscript and conceived of experiments.

ACKNOWLEDGMENTS

We thank Danny Carney and Hannah Lohr for technical assistance and support. We also thank the Riley Heart Research Center Group for discussion and helpful feedback. Furthermore, we thank Thomas Coate for kindly providing $EfnB2^{fx/fx}$ mice. Infrastructural support at the Herman B Wells Center is partially supported by the Riley Children's Foundation and the Carleton Buehl McCulloch Chair. Grant support for this work was provided by NIH grants 1R01HL120920-01, 1R01HL122123-01, and 1R0AR061392-03 (A.B.F.) and American Heart Association predoctoral fellowship 12PRE11700006 (N.J.V.).

Received: August 29, 2014
Revised: October 24, 2014
Accepted: November 13, 2014
Published: December 11, 2014

REFERENCES

Anderson, R., Becker, A., Macartney, F., Shinebourne, E., Wilkinson, J., and Tynan, M. (1979). Is "tricuspid atresia" a univentricular heart? Pediatr. Cardiol. *1*, 51–56.

Barnes, R.M., Firulli, B.A., VanDusen, N.J., Morikawa, Y., Conway, S.J., Cserjesi, P., Vincentz, J.W., and Firulli, A.B. (2011). Hand2 loss-of-function in Hand1-expressing cells reveals distinct roles in epicardial and coronary vessel development. Circ. Res. *108*, 940–949.

Benedito, R., Rocha, S.F., Woeste, M., Zamykal, M., Radtke, F., Casanovas, O., Duarte, A., Pytowski, B., and Adams, R.H. (2012). Notch-dependent VEGFR3 upregulation allows angiogenesis without VEGF-VEGFR2 signalling. Nature *484*, 110–114.

Bruneau, B.G. (2003). The developing heart and congenital heart defects: a make or break situation. Clin. Genet. *63*, 252–261.

Brutsaert, D.L. (2003). Cardiac endothelial-myocardial signaling: its role in cardiac growth, contractile performance, and rhythmicity. Physiol. Rev. *83*, 59–115.

Chen, H., Shi, S., Acosta, L., Li, W., Lu, J., Bao, S., Chen, Z., Yang, Z., Schneider, M.D., Chien, K.R., et al. (2004). BMP10 is essential for maintaining cardiac growth during murine cardiogenesis. Development *131*, 2219–2231.

Connerney, J., Andreeva, V., Leshem, Y., Muentener, C., Mercado, M.A., and Spicer, D.B. (2006). Twist1 dimer selection regulates cranial suture patterning and fusion. Dev. Dyn. *235*, 1345–1357.

Dixelius, J., Mäkinen, T., Wirzenius, M., Karkkainen, M.J., Wernstedt, C., Alitalo, K., and Claesson-Welsh, L. (2003). Ligand-induced vascular endothelial growth factor receptor-3 (VEGFR-3) heterodimerization with VEGFR-2 in primary lymphatic endothelial cells regulates tyrosine phosphorylation sites. J. Biol. Chem. *278*, 40973–40979.

Ferrara, N., Carver Moore, K., Chen, H., Dowd, M., Lu, L., O'Shea, K.S., Powell Braxton, L., Hillan, K.J., and Moore, M.W. (1996). Heterozygous embryonic lethality induced by targeted inactivation of the VEGF gene. Nature *380*, 439–442.

Firulli, B.A., Redick, B.A., Conway, S.J., and Firulli, A.B. (2007). Mutations within helix I of Twist1 result in distinct limb defects and variation of DNA binding affinities. J. Biol. Chem. *282*, 27536–27546.

Frensing, T., Kaltschmidt, C., and Schmitt-John, T. (2008). Characterization of a neuregulin-1 gene promoter: positive regulation of type I isoforms by NF-kappaB. Biochim. Biophys. Acta *1779*, 139–144.

Gerety, S.S., and Anderson, D.J. (2002). Cardiovascular ephrinB2 function is essential for embryonic angiogenesis. Development *129*, 1397–1410.

Go, A.S., Mozaffarian, D., Roger, V.L., Benjamin, E.J., Berry, J.D., Borden, W.B., Bravata, D.M., Dai, S., Ford, E.S., Fox, C.S., et al.; American Heart Association Statistics Committee and Stroke Statistics Subcommittee (2013). Heart disease and stroke statistics—2013 update: a report from the American Heart Association. Circulation *127*, e6–e245.

Grego-Bessa, J., Luna-Zurita, L., del Monte, G., Bolós, V., Melgar, P., Arandilla, A., Garratt, A.N., Zang, H., Mukouyama, Y.S., Chen, H., et al. (2007). Notch signaling is essential for ventricular chamber development. Dev. Cell *12*, 415–429.

Herbert, S.P., and Stainier, D.Y. (2011). Molecular control of endothelial cell behaviour during blood vessel morphogenesis. Nat. Rev. Mol. Cell Biol. *12*, 551–564.

Hoffman, J.I. (1995). Incidence of congenital heart disease: I. Postnatal incidence. Pediatr. Cardiol. *16*, 103–113.

Jiao, K., Langworthy, M., Batts, L., Brown, C.B., Moses, H.L., and Baldwin, H.S. (2006). Tgfbeta signaling is required for atrioventricular cushion mesenchyme remodeling during in vivo cardiac development. Development *133*, 4585–4593.

Kim, J.S., Virágh, S., Moorman, A.F., Anderson, R.H., and Lamers, W.H. (2001). Development of the myocardium of the atrioventricular canal and the vestibular spine in the human heart. Circ. Res. *88*, 395–402.

Kisanuki, Y.Y., Hammer, R.E., Miyazaki, J., Williams, S.C., Richardson, J.A., and Yanagisawa, M. (2001). Tie2-Cre transgenic mice: a new model for endothelial cell-lineage analysis in vivo. Dev. Biol. *230*, 230–242.

Kramer, R., Bucay, N., Kane, D.J., Martin, L.E., Tarpley, J.E., and Theill, L.E. (1996). Neuregulins with an Ig-like domain are essential for mouse myocardial and neuronal development. Proc. Natl. Acad. Sci. USA *93*, 4833–4838.

McFadden, D.G., McAnally, J., Richardson, J.A., Charité, J., and Olson, E.N. (2002). Misexpression of dHAND induces ectopic digits in the developing limb bud in the absence of direct DNA binding. Development *129*, 3077–3088.

Miquerol, L., Langille, B.L., and Nagy, A. (2000). Embryonic development is disrupted by modest increases in vascular endothelial growth factor gene expression. Development *127*, 3941–3946.

Osterwalder, M., Speziale, D., Shoukry, M., Mohan, R., Ivanek, R., Kohler, M., Beisel, C., Wen, X., Scales, S.J., and Christoffels, V.M. (2014). HAND2 targets define a network of transcriptional regulators that compartmentalize the early limb bud mesenchyme. Dev. Cell *31*, 345–357.

Pinto, A.R., Paolicelli, R., Salimova, E., Gospocic, J., Slonimsky, E., Bilbao-Cortes, D., Godwin, J.W., and Rosenthal, N.A. (2012). An abundant tissue macrophage population in the adult murine heart with a distinct alternatively-activated macrophage profile. PLoS ONE *7*, e36814.

Red-Horse, K., Ueno, H., Weissman, I.L., and Krasnow, M.A. (2010). Coronary arteries form by developmental reprogramming of venous cells. Nature *464*, 549–553.

Shawber, C.J., Funahashi, Y., Francisco, E., Vorontchikhina, M., Kitamura, Y., Stowell, S.A., Borisenko, V., Feirt, N., Podgrabinska, S., Shiraishi, K., et al. (2007). Notch alters VEGF responsiveness in human and murine endothelial cells by direct regulation of VEGFR-3 expression. J. Clin. Invest. *117*, 3369–3382.

Smart, N., Dubé, K.N., and Riley, P.R. (2009). Coronary vessel development and insight towards neovascular therapy. Int. J. Exp. Pathol. *90*, 262–283.

Svensson, E.C., Huggins, G.S., Lin, H., Clendenin, C., Jiang, F., Tufts, R., Dardik, F.B., and Leiden, J.M. (2000). A syndrome of tricuspid atresia in mice with a targeted mutation of the gene encoding Fog-2. Nat. Genet. *25*, 353–356.

Takeuchi, J.K., Ohgi, M., Koshiba-Takeuchi, K., Shiratori, H., Sakaki, I., Ogura, K., Saijoh, Y., and Ogura, T. (2003). Tbx5 specifies the left/right ventricles and ventricular septum position during cardiogenesis. Development *130*, 5953–5964.

Tammela, T., Zarkada, G., Wallgard, E., Murtomäki, A., Suchting, S., Wirzenius, M., Waltari, M., Hellström, M., Schomber, T., Peltonen, R., et al. (2008). Blocking VEGFR-3 suppresses angiogenic sprouting and vascular network formation. Nature *454*, 656–660.

Tian, X., Hu, T., Zhang, H., He, L., Huang, X., Liu, Q., Yu, W., He, L., Yang, Z., Zhang, Z., et al. (2013). Subepicardial endothelial cells invade the embryonic ventricle wall to form coronary arteries. Cell Res. *23*, 1075–1090.

Tsuchihashi, T., Maeda, J., Shin, C.H., Ivey, K.N., Black, B.L., Olson, E.N., Yamagishi, H., and Srivastava, D. (2011). Hand2 function in second heart field progenitors is essential for cardiogenesis. Dev. Biol. *351*, 62–69.

VanDusen, N.J., Vincentz, J.W., Firulli, B.A., Howard, M.J., Rubart, M., and Firulli, A.B. (2014). Loss of Hand2 in a population of Periostin lineage cells results in pronounced bradycardia and neonatal death. Dev. Biol. *388*, 149–158.

Verzi, M.P., McCulley, D.J., De Val, S., Dodou, E., and Black, B.L. (2005). The right ventricle, outflow tract, and ventricular septum comprise a restricted expression domain within the secondary/anterior heart field. Dev. Biol. *287*, 134–145.

Vincentz, J.W., Barnes, R.M., Rodgers, R., Firulli, B.A., Conway, S.J., and Firulli, A.B. (2008). An absence of Twist1 results in aberrant cardiac neural crest morphogenesis. Dev. Biol. *320*, 131–139.

Wu, B., Zhang, Z., Lui, W., Chen, X., Wang, Y., Chamberlain, A.A., Moreno-Rodriguez, R.A., Markwald, R.R., O'Rourke, B.P., Sharp, D.J., et al. (2012). Endocardial cells form the coronary arteries by angiogenesis through myocardial-endocardial VEGF signaling. Cell *151*, 1083–1096.

Wythe, J.D., Dang, L.T., Devine, W.P., Boudreau, E., Artap, S.T., He, D., Schachterle, W., Stainier, D.Y., Oettgen, P., Black, B.L., et al. (2013). ETS factors regulate Vegf-dependent arterial specification. Dev. Cell *26*, 45–58.

Yamagishi, H., Olson, E.N., and Srivastava, D. (2000). The basic helix-loop-helix transcription factor, dHAND, is required for vascular development. J. Clin. Invest. *105*, 261–270.